

SUPPORTING INFORMATION

On Describing the Optoelectronic Characteristics of Poly(benzodithiophene-*co*-quinoxaline)-Fullerene Complexes: The Influence of Optimally Tuned Density Functionals

Tuuya Kastinen^{*,a}, Mika Niskanen^{a,b}, Chad Risko^c, Oana Cramariuc^{*,d}, and Terttu I. Hukka^{*,a}

^aDepartment of Chemistry and Bioengineering, Tampere University of Technology, P.O. Box 541, FI-33101, Tampere, Finland. E-mail: tuuya.kastinen@tut.fi, terttu.hukka@tut.fi

^bDepartment of Physics, Imperial College London, South Kensington Campus, London SW7 2AZ, UK

^cDepartment of Chemistry and Center for Applied Energy Research, University of Kentucky, Lexington, Kentucky 40506-0055, USA

^dDepartment of Physics, Tampere University of Technology, P.O. Box 692, FI-33101, Tampere, Finland. E-mail: oana.cramariuc@tut.fi

Contents

Relaxed PES scans of the monomer model	S2
Effect of the backbone structure on the electronic properties of the trimer	S2
Structures of the O3p-PC ₇₁ BM models	S2–S4
Total and relative energies of the copolymer models	S4
Bond numbers and bond length differences for the copolymer models	S4–S5
Electronic and optical properties of O3-anti	S5–S7
Electronic and optical properties of the fullerene derivatives	S7–S8
Potential energy scans of the O3p-PC ₇₁ BM models	S9
Interaction energies of the O3p-PC ₇₁ BM models with the intermolecular distance of 3.5 Å	S9
Excited state properties of the O3p-PC ₇₁ BM models with the constant intermolecular distance of 3.5 Å	S10–S12
Excited state properties of the O3p-PC ₇₁ BM models with the minimized intermolecular distances	S13–S15
UV-Vis absorption spectra of O3p, PC ₇₁ BM, and the models 3a and 3b	S16
Natural transition orbitals of the vertical model 3a at the intermolecular distance of 3.5 Å	S17–S18
Natural transition orbitals of the horizontal model 3b at the intermolecular distance of 3.5 Å	S19

Relaxed PES scans of the monomer model

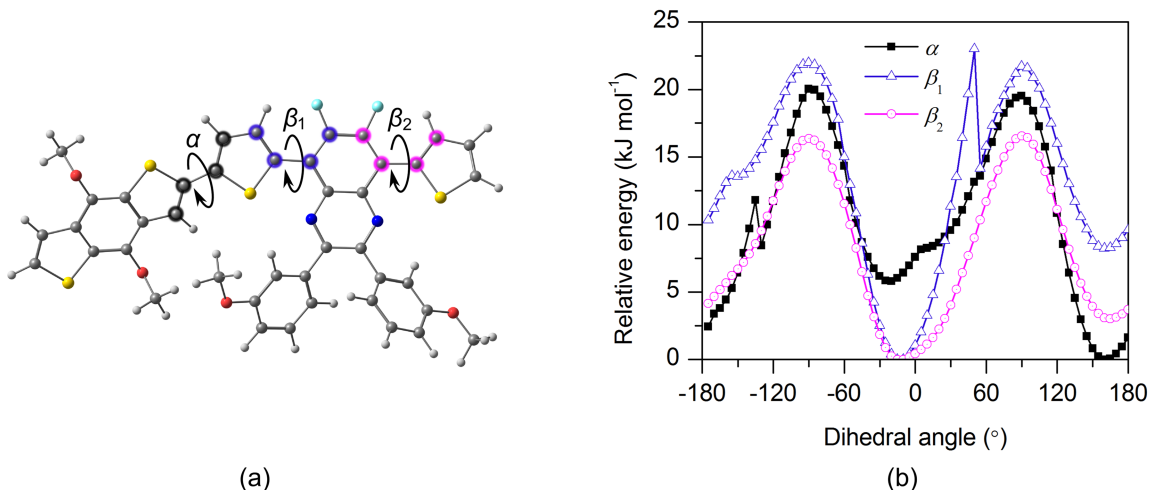


Figure S1 Representations of (a) the scanned dihedral angles between donor, thiophene, and acceptor moieties within one CRU, i.e. within the monomer model, of the studied D–A copolymer and (b) the corresponding PES curves. The relaxed PES scans were carried out at the B3LYP/6-31G** level of theory.

Effect of the backbone structure on the electronic properties of the trimer

In O3p, the hexyloxyphenyl side groups of the quinoxaline acceptor unit were replaced by hydrogen atoms to reduce the computational cost. Additionally, the backbone of the trimer was planarized. These modifications have small effects on the electronic properties of the trimer of the studied D–A copolymer (see Table S1), namely both the HOMO and LUMO energies of O3p are stabilized with respect to those of O3-anti, in which the methoxyphenyl side groups were used in the acceptor units. Additionally, the HOMO–LUMO gap of O3p is 0.1 eV smaller than that of O3-anti.

Table S1 HOMO, LUMO, and HOMO–LUMO gap ($E_{\text{HOMO-LUMO}}$) energies of the fully optimized O3-anti and planarized O3p ($n = 3$) calculated with DFT at the B3LYP/6-31G** level of theory.

Model	HOMO (eV)	LUMO (eV)	$E_{\text{HOMO-LUMO}}$ (eV)
O3-anti	-4.84	-2.69	2.15
O3p	-4.87	-2.82	2.05

Structures of the O3p–PC₇₁BM models

The α isomer¹ of PC₇₁BM was employed in all O3p–PC₇₁BM models. In **1a** and **3a** (Figure 3 in the main article), the furthermost benzene ring (the C53-C54-C55-C56-C68-C67 ring²) of PC₇₁BM from its phenyl butyric acid methyl ester group (attached to the C8 and C25 atoms of C₇₀ in the α isomer¹) was superposed on the benzene ring of O3p, whereas in **2a** the centroid of the particular benzene ring (the C53-C54-C55-C56-C68-C67 ring²) of PC₇₁BM was superposed on the centroid of the thiophene ring of the trimer. In **1b–3b** (Figure S3), the benzene ring (or its centroid) on the side of PC₇₁BM (the C61-C62-C63-C64-C65-C70 ring²) was superposed on the same units of the trimer

as in **1a–3a**. See Figure S4 for the positions of the superposed rings and centroids in O3p and PC₇₁BM.

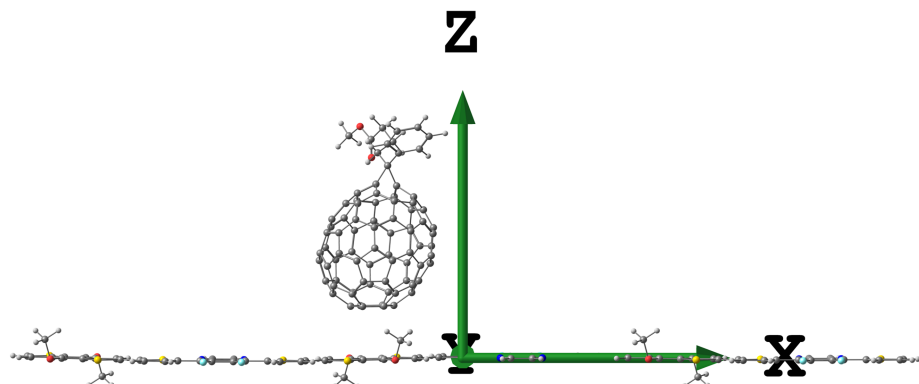


Figure S2 Orientation of the *x*, *y*, and *z* axis in all eD–eA models. In Models **1b–3b**, PC₇₁BM was oriented horizontally (i.e. along the *x* axis) above the trimer.

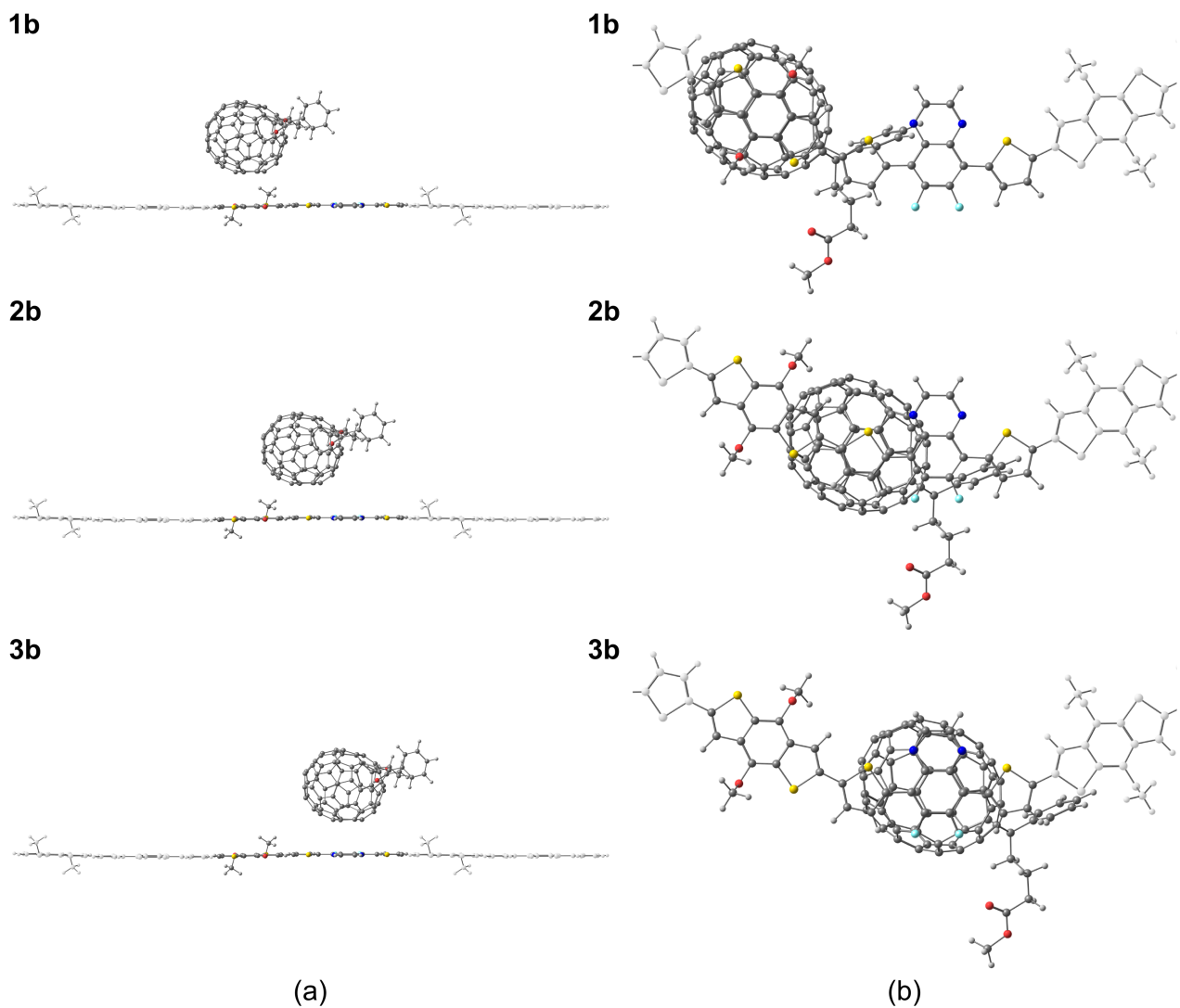


Figure S3 Horizontal eD–eA models represented from (a) the side and (b) the bottom of the models. In the models, PC₇₁BM (eA), is positioned horizontally on the donor (**1b**), thiophene spacer (**2b**), or acceptor (**3b**) unit of the planarized O3p trimer model (eD) of the D–A copolymer.

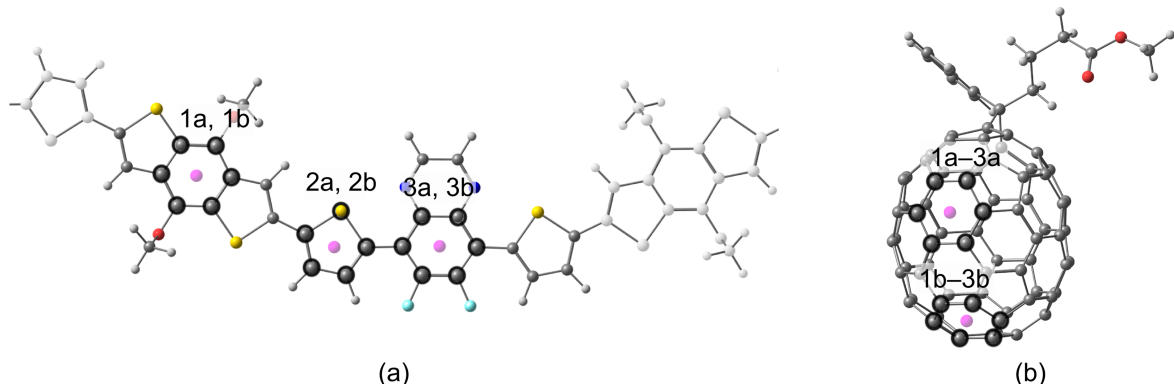


Figure S4 Positions of the rings and centroids in the Models 1a–3a and 1b–3b, which were used to superpose (a) the O3p trimer (only the innermost CRU is presented wholly in the figure) and (b) PC₇₁BM.

Total and relative energies of the copolymer models

Table S2 Total (Hartree) and relative energies (kJ mol⁻¹) of the *syn*- and *anti*-conformations of the monomer and trimer models ($n = 1, 3$) and periodic models ($n = \infty$) calculated at the B3LYP/6-31G** level of theory. Relative energies have been calculated as the energy difference between the *syn*- and *anti*-conformations of the same size.

Functional	ω (bohr ⁻¹)	n	Total energy (Hartree)		Relative energy (kJ mol ⁻¹)
			<i>syn</i>	<i>anti</i>	
B3LYP	-	1	-4282.2848190	-4282.2848190	0.00
B3LYP		3	-11920.2088306	-11920.2137256	12.85
ω B97X	0.30		-11456.2350030	-11456.2397930	12.58
OT- ω B97X	0.10		-11459.1190224	-11459.1223707	8.79
B3LYP	-	∞^a	-11456.8837355	-11456.8918492	21.30
ω B97X	0.30		-11455.0502302	-11455.0595564	24.49
OT- ω B97X	0.10		-11457.9269395	-11457.9332040	16.45

^aThe trimer was used as the CRU.

Bond numbers and bond length differences for the copolymer models

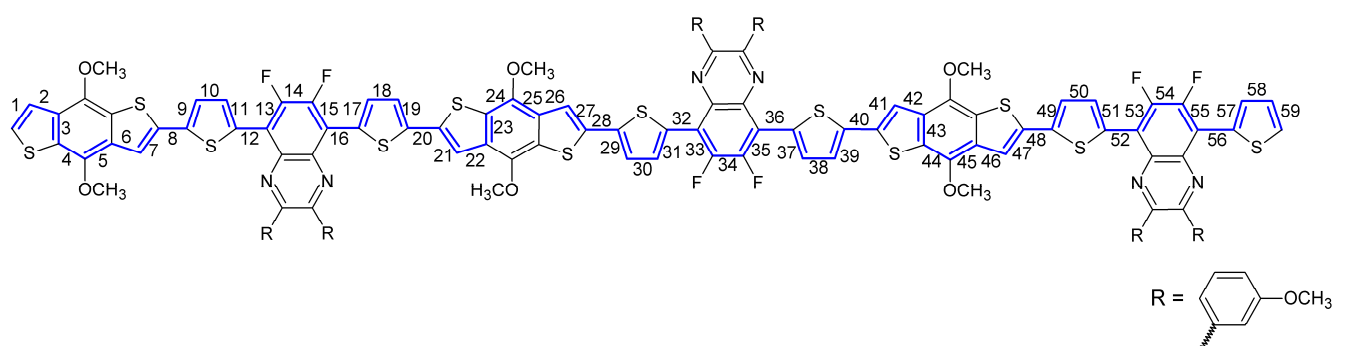


Figure S5 Bond numbers along the conjugation path of O3-anti/P-anti.

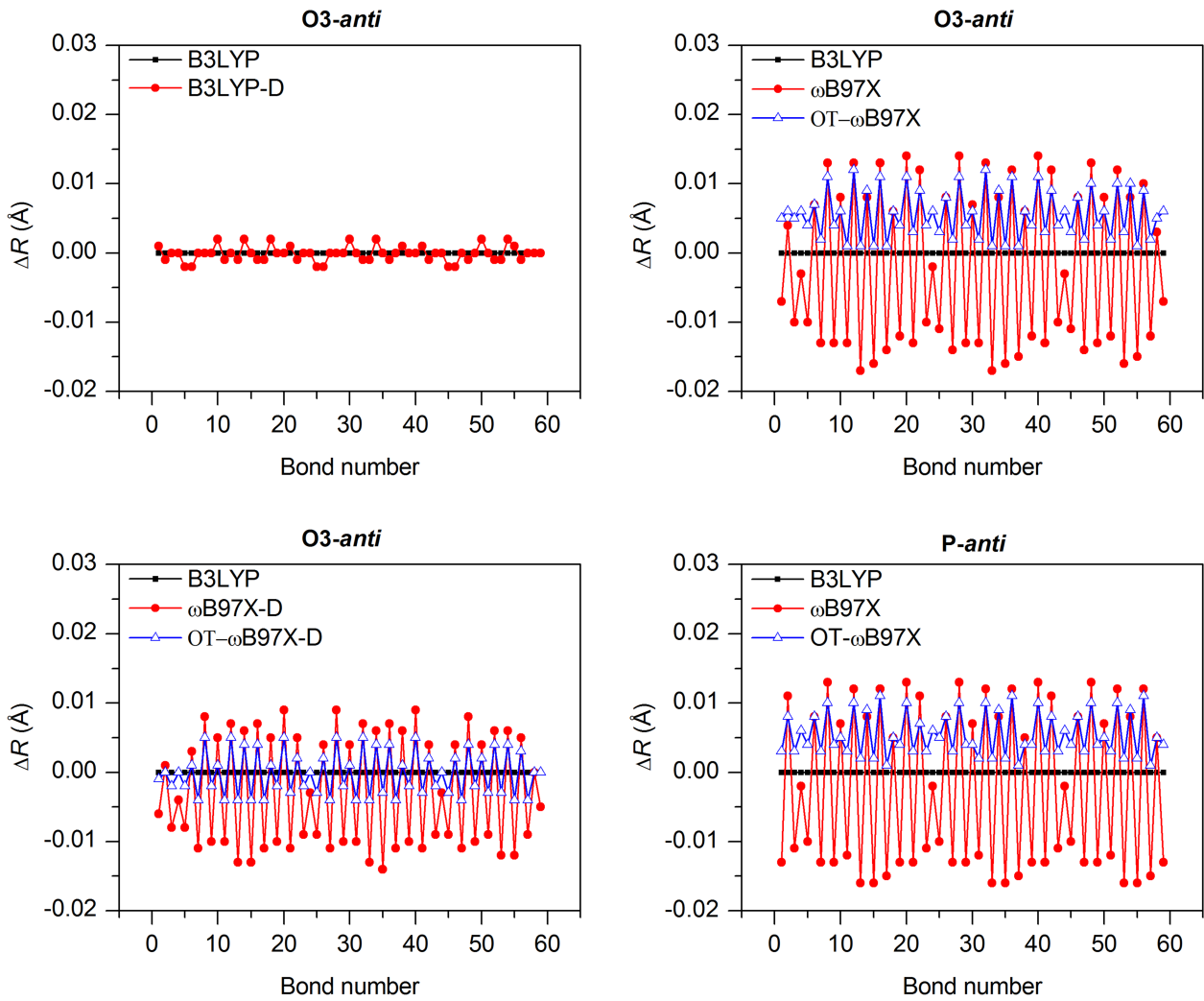


Figure S6 Differences in bond lengths (ΔR , Å) calculated using the 6-31G** basis set with different functionals relative to the B3LYP values of the optimized O3-*anti* ($n = 3$) and P-*anti* ($n = \infty$) plotted as the function of the bond number. The ΔR values were calculated as $R(\text{functional}) - R(\text{B3LYP})$.

Electronic and optical properties of O3-*anti*

In this study, we employed the ground-state geometries of the studied compounds optimized at the same level of theory as their electronic and optical properties have been calculated. For the sake of comparison, the oligomeric results calculated at the B3LYP-optimized O3-*anti* geometry are presented in Table S3. Similarly, the results calculated at the B3LYP-optimized geometries of PC₆₁BM and PC₇₁BM are presented in Tables S5 and S6, respectively. In general, the smaller gap values and smaller, i.e. red-shifted vertical transition energies (ca. 0.0–0.4 eV), are obtained with the B3LYP-optimized geometries when compared to those obtained with the geometries optimized with other functionals (see Tables 4–6 in the main article).

Table S3 HOMO, LUMO, and HOMO–LUMO gap ($E_{\text{HOMO-LUMO}}$) energies calculated with DFT and the vertical transition energies ($E_{\text{vert, S1}}$), oscillator strengths (f), and electronic configurations of O3-*anti* ($n = 3$) calculated with TDDFT using different functionals and the 6-31G** basis set at the B3LYP/6-31G** optimized geometry. The TDDFT values calculated in 1,2-dichlorobenzene are presented in parentheses.

Functional	ω (bohr ⁻¹)	HOMO (eV)	LUMO (eV)	$E_{\text{HOMO-LUMO}}$ (eV)	$E_{\text{vert, S1}}$ (eV)	f	Electronic configuration ^b
B3LYP	–	-4.84	-2.69	2.15	1.82 (1.83)	2.95 (3.30)	H → L, 90% (88%) H-1 → L+1, 7% (7%)
B3LYP-D	-	-4.83	-2.68	2.15	– ^c	– ^c	– ^c
ω B97X	0.30	-6.87	-1.04	5.83	2.74 (2.73)	4.69 (4.90)	H → L, 45% (45%) H-1 → L+1, 15% (15%)
ω B97X-D	0.20	-6.54	-1.25	5.29	2.56 (2.54)	4.52 (4.77)	H → L, 50% (49%) H-1 → L+1, 16% (16%)
OT- ω B97X	0.10	-5.58	-1.55	4.03	2.13 (2.13)	3.73 (4.09)	H → L, 62% (62%) H-1 → L+1, 17% (16%)
OT- ω B97X-D	0.09	-5.73	-1.68	4.05	2.16 (2.16)	3.86 (4.21)	H → L, 63% (62%) H-1 → L+1, 17% (16%)

^aCorresponding DFT and TDDFT calculations were carried out at the same levels of theory. ^bOnly the two largest contributing electronic configurations are included. ^cComputationally too demanding. The experimental cyclic voltammogram (CV) values³ to compare with the calculated energy values are -5.52 eV (HOMO) -3.30 eV (LUMO), respectively, giving an electrochemical gap of 2.22 eV. The absorption maximum³ (in 1,2-dichlorobenzene) is at 2.24 eV (553 nm).

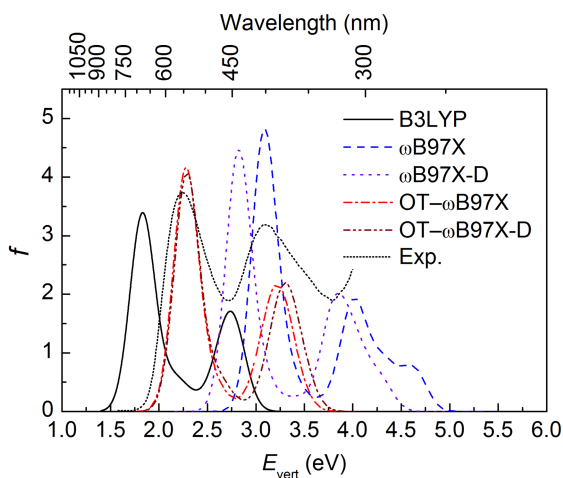


Figure S7 UV-vis absorption spectra of O3-*anti* ($n = 3$) calculated in 1,2-dichlorobenzene with TDDFT employing different functionals and the 6-31G** basis set. The geometries were optimized with DFT using the corresponding level of theory. The (scaled) digitized experimental absorption spectrum³ is also presented for comparison.

Table S4. Contributions (%)^a of the charge densities of the BDT donor, thiophene spacer (T), and quinoxaline acceptor (Q) units to the main and second (in parentheses) NTO pairs^b corresponding to the S₀→S₁ transition of O3-anti ($n = 3$).

Functional	hole			electron		
	BDT	T	Q	BDT	T	Q
ω B97X	27 (21)	46 (48)	27 (31)	20 (15)	32 (32)	48 (53)
ω B97X-D	28 (23)	46 (48)	26 (29)	18 (15)	29 (29)	53 (56)
OT- ω B97X-D	37 (31)	44 (47)	19 (22)	17 (15)	25 (24)	58 (61)

^aCalculated via C-SPA⁴. ^bThe NTOs were determined with TDDFT employing different functionals and 6-31G**. The contributions and NTOs calculated with B3LYP and OT- ω B97X are presented in Figure 6 of the main article.

Electronic and optical properties of the fullerene derivatives

Table S5 HOMO, LUMO, and HOMO–LUMO gap ($E_{\text{HOMO-LUMO}}$) energies of PC₆₁BM calculated with DFT^a and the vertical transition energies ($E_{\text{vert, max}}$), oscillator strengths (f), and electronic configurations of the excitation corresponding to the absorption maximum in the UV-vis spectrum calculated with TDDFT^a employing different functionals and the 6-31G** basis set. The TDDFT values calculated in toluene are presented in parentheses.

Functional	ω (bohr ⁻¹)	HOMO (eV)	LUMO (eV)	$E_{\text{HOMO-LUMO}}$ (eV)	$E_{\text{vert, max}}$ (eV)	f	Electronic configuration^b
B3LYP	–	-5.56	-3.00	2.56	3.50 (3.50)	0.01 (0.02)	H-1 → L+4, 31% (31%) H-11 → L, 27% (25%)
B3LYP-D		-5.56	-3.00	2.56	3.50 (3.50)	0.01 (0.02)	H-1 → L+4, 31% (31%) H-11 → L, 27% (25%)
ω B97X	0.30	-7.61	-1.43	6.18	4.73 (4.66)	0.63 (1.10)	H-2 → L+3, 26% (25%) H-1 → L+4, 14% (14%)
ω B97X-D	0.20	-7.35	-1.63	5.72	4.44 (4.39)	0.41 (0.77)	H-2 → L+3, 30% (27%) H-1 → L+4, 14% (14%)
OT- ω B97X	0.16	-6.94	-1.66	5.28	4.15 (4.12)	0.14 (0.41)	H-2 → L+3, 27% (29%) H-8 → L, 13% (17%)
OT- ω B97X-D	0.15	-7.07	-1.77	5.30	4.20 (4.17)	0.16 (0.42)	H-2 → L+3, 29% (28%) H-8 → L, 13% (16%)

^aCorresponding DFT and TDDFT calculations were carried out at the same levels of theory using the B3LYP/6-31G** optimized geometry in all calculations. ^bOnly the two largest contributing electronic configurations are included. Experimental values^{5,6} of IE and EA of PC₆₁BM (in gas-phase) are 7.17±0.04⁷ eV and 2.63 eV⁸ eV, respectively. The experimental absorption maximum¹ (in toluene) is at ca. 3.65 eV (ca. 340 nm).

Table S6 HOMO, LUMO, and HOMO–LUMO gap ($E_{\text{HOMO-LUMO}}$) energies of PC₇₁BM calculated with DFT^a and the vertical transition energies ($E_{\text{vert, max}}$), oscillator strengths (f), and electronic configurations of the excitation corresponding to the first absorption maximum in the UV-vis spectrum calculated with TDDFT^a employing different functionals and the 6-31G** basis set. The TDDFT values calculated in toluene are presented in parentheses.

Functional	ω (bohr ⁻¹)	HOMO (eV)	LUMO (eV)	$E_{\text{HOMO-LUMO}}$ (eV)	$E_{\text{vert, max}}$ (eV)	f	Electronic configuration ^b
B3LYP	–	-5.52	-2.98	2.54	2.37 (2.34)	0.04 (0.06)	H-1 → L+1, 37% H-2 → L+2, 18% (H-2 → L+1, 71%) (H-5 → L, 6%)
B3LYP-D	–	-5.52	-2.98	2.54	2.37 (2.34)	0.04 (0.06)	H-1 → L+1, 37% H-2 → L+2, 18% (H-2 → L+1, 71%) (H-5 → L, 6%)
ω B97X	0.30	-7.32	-1.52	5.80	2.84 (2.82)	0.06 (0.12)	H → L+2, 56% (57%) H-3 → L, 8% (H-1 → L, 9%)
ω B97X-D	0.20	-7.12	-1.71	5.41	2.68 (2.67)	0.04 (0.09)	H → L+2, 71% (71%) H-3 → L, 5% (5%)
OT- ω B97X	0.14	-6.64	-1.77	4.87	2.55 (2.54)	0.04 (0.07)	H-1 → L+1, 59% (61%) H-1 → L, 12% (15%)
OT- ω B97X-D	0.13	-6.77	-1.88	4.89	2.58 (2.57)	0.05 (0.07)	H-1 → L+1, 61% (63%) H-1 → L, 11% (13%)

^aCorresponding DFT and TDDFT calculations were carried out at the same levels of theory using the B3LYP/6-31G** optimized geometry in all calculations. ^bOnly the two largest contributing electronic configurations are included. Experimental values^{5,6} of IE, EA, and fundamental gap of PC₇₁BM (measured from films) are 5.9 eV, 3.8 eV, and 2.1 eV, respectively. The experimental absorption maximum¹ (in toluene) is at ca. 2.68 eV (ca. 462 nm).

Potential energy curves of the O3p–PC₇₁BM models

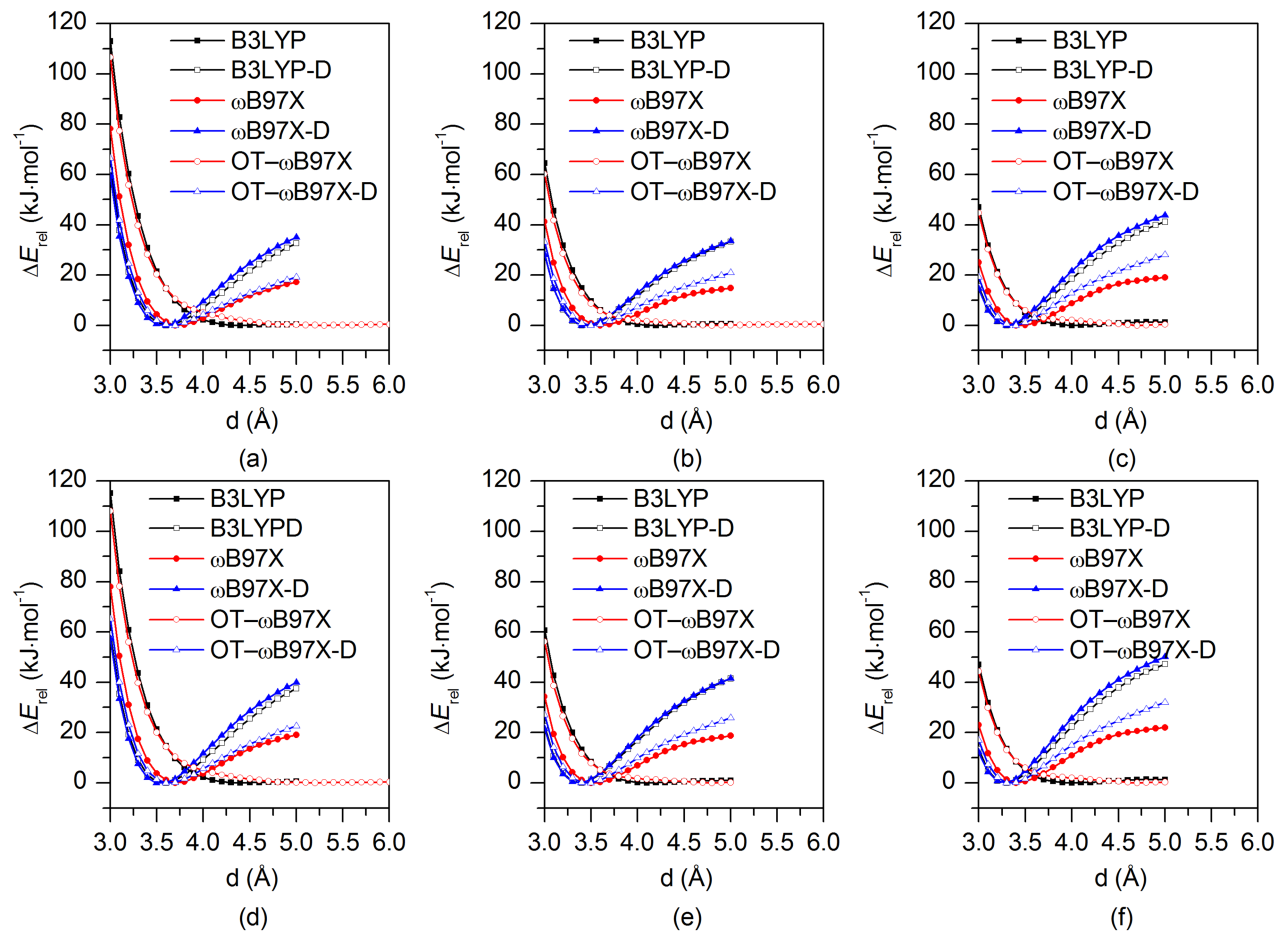


Figure S8 One-dimensional single point (rigid) potential energy scans of the distance between the planarized O3p trimer and PC₇₁BM (d , Å) for the models: (a) **1a**, (b) **2a**, (c) **3a**, (d) **1b**, (e) **2b**, and (f) **3b**.

Interaction energies of the O3p–PC₇₁BM models with the intermolecular distance of 3.5 Å

Table S7 Interaction energies (kJ mol⁻¹)^a between the planarized O3p and PC₇₁BM in the O3p–PC₇₁BM models calculated with various functionals and the 6-31G** basis set at the intermolecular distance of 3.5 Å.

Functional	ω (bohr ⁻¹)	Model					
		1a	2a	3a	1b	2b	3b
B3LYP	–	20.66	9.28	3.99	20.69	7.46	3.5
B3LYP-D	–	-50.05	-47.49	-53.15	-57.52	-56.95	-60.1
ω B97X	0.30	-15.26	-14.87	-19.44	-17.70	-19.67	-22.2
ω B97X-D	0.20	-52.39	-47.20	-54.62	-59.54	-56.28	-61.3
OT- ω B97X	0.13	20.15	8.31	5.44	19.91	7.18	5.1
OT- ω B97X-D	0.12	-33.45	-34.50	-40.91	-39.40	-41.52	-46.3

^aCalculated using eq. 6 in the main article.

Excited state properties of the O3p–PC₇₁BM models with the intermolecular distance of 3.5 Å

Table S8 Oscillator strengths for the first 10 singlet excited states of the O3p–PC₇₁BM models with the intermolecular distance of 3.5 Å between the planarized O3p trimer and PC₇₁BM.

Model	Functional	S ₁	S ₂	S ₃	S ₄	S ₅	S ₆	S ₇	S ₈	S ₉	S ₁₀
1a	B3LYP	0.04	0.09	2.55	0.56	0.01	0.03	0.00	0.00	0.03	0.01
	ωB97X	0.00	5.24	0.08	0.07	0.05	0.02	0.00	0.01	0.03	0.01
	ωB97X-D	0.00	5.03	0.05	0.06	0.03	0.01	0.01	0.01	0.04	(0.01)
	OT-ωB97X	0.01	4.34	0.05	0.05	0.04	0.00	0.01	0.01	0.09	0.03
	OT-ωB97X-D	0.01	4.48	0.04	0.04	0.04	0.00	0.01	0.01	0.10	0.03
2a	B3LYP	0.17	0.24	1.66	1.18	0.00	0.03	0.01	0.01	0.00	(0.01)
	ωB97X	0.00	4.77	0.33	0.06	0.09	0.02	0.01	0.04	0.03	0.00
	ωB97X-D	0.01	4.74	0.11	0.07	0.06	0.01	0.05	0.02	0.06	0.01
	OT-ωB97X	0.03	4.09	0.03	0.11	0.00	0.15	0.01	0.05	(0.08)	0.16
	OT-ωB97X-D	0.03	4.22	0.03	0.10	0.00	0.15	0.02	0.06	(0.09)	0.14
3a	B3LYP	0.17	0.10	0.50	2.48	0.02	0.01	0.06	0.00	0.00	(0.01)
	ωB97X	0.00	4.53	0.54	0.10	0.07	0.03	0.01	0.05	0.03	0.00
	ωB97X-D	0.00	4.67	0.18	0.06	0.08	0.01	0.03	0.06	0.06	0.00
	OT-ωB97X	0.02	4.05	0.06	0.10	0.01	0.18	0.03	0.08	0.17	0.02
	OT-ωB97X-D	0.02	4.18	0.06	0.09	0.01	0.13	0.07	0.10	0.17	0.02
1b	B3LYP	0.02	0.00	2.93	0.17	0.02	0.03	0.00	0.13	0.00	0.01
	ωB97X	0.00	5.15	0.09	0.14	0.02	0.03	0.00	0.01	0.02	0.01
	ωB97X-D	0.00	4.97	0.04	0.11	0.02	0.01	0.03	0.00	0.04	0.00
	OT-ωB97X	0.00	4.31	0.01	0.05	0.05	0.00	0.02	0.00	0.11	(0.04)
	OT-ωB97X-D	0.01	4.44	0.01	0.04	0.05	0.00	0.02	0.00	0.12	(0.04)
2b	B3LYP	0.08	0.06	2.73	0.31	0.00	0.04	0.00	0.03	0.01	0.01
	ωB97X	0.00	4.95	0.12	0.14	0.03	0.03	0.00	0.04	0.06	0.00
	ωB97X-D	0.00	4.79	0.05	0.12	0.01	0.01	0.03	0.05	0.07	0.00
	OT-ωB97X	0.01	4.14	0.01	0.16	0.06	0.00	0.01	0.00	0.09	0.05
	OT-ωB97X-D	0.02	4.26	0.01	0.13	0.07	0.00	0.01	0.00	(0.08)	0.04
3b	B3LYP	0.14	0.11	0.37	2.64	0.00	0.01	0.04	0.00	0.00	0.02
	ωB97X	0.00	4.81	0.25	0.10	0.04	0.05	0.01	0.04	0.07	0.00
	ωB97X-D	0.00	4.76	0.07	0.09	0.03	0.01	0.07	0.03	0.08	0.02
	OT-ωB97X	0.00	4.02	0.01	0.17	0.03	0.24	0.03	0.00	0.06	0.04
	OT-ωB97X-D	0.01	4.17	0.01	0.14	0.03	0.25	0.03	0.00	0.06	0.04

The oscillator strengths that are greater than or equal to 0.10 are in bold. The oscillator strengths of the excited singlet states that did not converge are in parenthesis.

Table S9 Vertical transition energies (eV) for the first 10 singlet excited states of the O3p–PC₇₁BM models with the intermolecular distance of 3.5 Å between the planarized O3p trimer and PC₇₁BM.

Model	Functional	S ₁	S ₂	S ₃	S ₄	S ₅	S ₆	S ₇	S ₈	S ₉	S ₁₀
1a	B3LYP	1.62	1.68	1.73	1.77	1.90	1.92	1.95	2.01	2.01	2.02
	ω B97X	2.40	2.67	2.68	2.83	2.86	2.93	2.94	2.96	3.02	3.04
	ω B97X-D	2.28	2.48	2.52	2.66	2.68	2.73	2.76	2.78	2.81	(2.85)
	OT- ω B97X	2.12	2.18	2.25	2.33	2.36	2.39	2.45	2.46	2.50	2.52
	OT- ω B97X-D	2.15	2.21	2.28	2.38	2.39	2.43	2.49	2.50	2.54	2.55
2a	B3LYP	1.61	1.68	1.73	1.77	1.86	1.91	1.92	2.00	2.00	(2.02)
	ω B97X	2.40	2.66	2.68	2.83	2.86	2.92	2.94	2.95	3.02	3.03
	ω B97X-D	2.28	2.47	2.51	2.66	2.68	2.73	2.77	2.77	2.81	2.85
	OT- ω B97X	2.12	2.17	2.25	2.36	2.39	2.41	2.45	2.46	(2.51)	2.52
	OT- ω B97X-D	2.15	2.20	2.29	2.39	2.43	2.45	2.48	2.50	(2.55)	2.56
3a	B3LYP	1.57	1.64	1.71	1.76	1.81	1.88	1.92	1.95	2.00	(2.03)
	ω B97X	2.40	2.66	2.68	2.83	2.86	2.92	2.93	2.95	3.02	3.03
	ω B97X-D	2.29	2.47	2.52	2.67	2.68	2.73	2.77	2.78	2.81	2.85
	OT- ω B97X	2.12	2.18	2.25	2.36	2.39	2.44	2.45	2.47	2.51	2.53
	OT- ω B97X-D	2.15	2.20	2.28	2.39	2.42	2.48	2.48	2.51	2.55	2.56
1b	B3LYP	1.63	1.69	1.72	1.79	1.92	1.92	1.97	1.99	2.01	2.02
	ω B97X	2.39	2.66	2.68	2.82	2.86	2.91	2.92	2.95	3.00	3.03
	ω B97X-D	2.28	2.48	2.51	2.65	2.69	2.71	2.73	2.77	2.79	2.85
	OT- ω B97X	2.12	2.18	2.24	2.27	2.36	2.38	2.44	2.45	2.51	(2.53)
	OT- ω B97X-D	2.15	2.20	2.28	2.31	2.39	2.41	2.48	2.49	2.54	(2.56)
2b	B3LYP	1.62	1.68	1.73	1.78	1.88	1.92	1.94	2.01	2.01	2.03
	ω B97X	2.40	2.66	2.68	2.82	2.86	2.91	2.93	2.95	3.00	3.03
	ω B97X-D	2.29	2.47	2.52	2.66	2.69	2.72	2.75	2.78	2.79	2.85
	OT- ω B97X	2.12	2.18	2.25	2.34	2.36	2.38	2.44	2.46	2.51	2.53
	OT- ω B97X-D	2.15	2.20	2.29	2.38	2.40	2.42	2.48	2.49	(2.55)	2.57
3b	B3LYP	1.59	1.64	1.74	1.76	1.83	1.87	1.92	1.98	2.00	2.03
	ω B97X	2.40	2.66	2.68	2.83	2.86	2.92	2.94	2.96	3.01	3.03
	ω B97X-D	2.29	2.48	2.51	2.66	2.68	2.73	2.76	2.78	2.80	2.85
	OT- ω B97X	2.12	2.18	2.25	2.35	2.38	2.40	2.45	2.47	2.52	2.53
	OT- ω B97X-D	2.15	2.20	2.28	2.38	2.42	2.44	2.48	2.50	2.55	2.56

The transitions, whose oscillator strengths (Table S8) are greater than or equal to 0.10, are in bold. The values of the excited singlet states that did not converge are in parenthesis.

Table S10 Nature of the first 10 singlet excited states of the O3p–PC₇₁BM models with the intermolecular distance between the planarized O3p trimer and PC₇₁BM of 3.5 Å.

Model	Functional	S ₁	S ₂	S ₃	S ₄	S ₅	S ₆	S ₇	S ₈	S ₉	S ₁₀
1a	B3LYP	PCT	PCT	CT	CT	PCT	LT	PCT	LF	CT	CT
	ωB97X	LF	LT	LF	LF	LT	LF	LF	LF	LF	LF
	ωB97X-D	LF	LT	LF	LT	LF	LF	LF	LF	LF	(LF)
	OT-ωB97X	LF	LT	LF	CT	LT	LF	LF	LF	CT	LF
	OT-ωB97X-D	LF	LT	LF	CT	CT	LF	LF	LF	CT	LF
2a	B3LYP	PCT	PCT	CT	CT	PCT	CT	CT	CT	LF	(LF)
	ωB97X	LF	LT	LF	LF	LT	LF	LF	LF	LF	LF
	ωB97X-D	LF	LT	LF	LT	LF	LF	LF	LF	LF	LF
	OT-ωB97X	LF	LT	LF	LT	LF	CT	LF	LF	(LF)	CT
	OT-ωB97X-D	LF	LT	LF	LT	LF	CT	LF	LF	(LF)	CT
3a	B3LYP	PCT	PCT	CT	CT	PCT	PCT	LT	PCT	LF	(LF)
	ωB97X	LF	LT	LF	LF	LT	LF	LF	LF	LF	LF
	ωB97X-D	LF	LT	LF	LT	LF	LF	LF	LF	LF	LF
	OT-ωB97X	LF	LT	LF	LT	LF	CT	LF	LF	LF	LF
	OT-ωB97X-D	LF	LT	LF	LT	LF	CT	CT	LF	LF	LF
1b	B3LYP	PCT	PCT	LT	PCT	PCT	LT	PCT	LT	LF	LF
	ωB97X	LF	LT	LF	LF	LT	LF	LF	LF	LF	LF
	ωB97X-D	LF	LT	LF	LT	LF	LF	CT	LF	LF	LF
	OT-ωB97X	LF	LT	CT	CT	LT	LF	LF	LF	LF	(LF)
	OT-ωB97X-D	LF	LT	LF	CT	LT	LF	LF	LF	LF	(LF)
2b	B3LYP	PCT	PCT	CT	PCT	PCT	LT	PCT	CT	LF	LF
	ωB97X	LF	LT	LF	LF	LT	LF	LF	LF	LF	LF
	ωB97X-D	LF	LT	LF	LT	LF	LF	LF	LF	LF	LF
	OT-ωB97X	LF	LT	LF	CT	CT	LF	LF	LF	LF	LF
	OT-ωB97X-D	LF	LT	LF	CT	CT	LF	LF	LF	(LF)	LF
3b	B3LYP	PCT	PCT	PCT	CT	PCT	PCT	LT	PCT	LF	LF
	ωB97X	LF	LT	LF	LF	LT	LF	LF	LF	LF	LF
	ωB97X-D	LF	LT	LF	LT	LF	LF	LF	LF	LF	LF
	OT-ωB97X	LF	LT	LF	CT	LF	CT	LF	LF	LF	LF
	OT-ωB97X-D	LF	LT	LF	LT	LF	CT	LF	LF	LF	LF

Only the NTO pair with the largest λ , i.e. the fraction of the NTO pair contribution to the particular excitation has been considered. The transitions, whose oscillator strengths (Table S8) are greater than or equal to 0.10, are in bold. The results of the excited singlet states that did not converge are in parenthesis. PCT: ‘pure’ charge transfer from the O3p trimer to PC₇₁BM, i.e. ≥ 90 percentage points (pp) of the electron density was transferred; CT: charge transfer from the O3p trimer to PC₇₁BM, i.e. 10 pp > of the electron density > 90 pp was transferred; LT: local excitation in the O3p trimer. LF: local excitation in PC₇₁BM. The threshold was 10 pp, i.e. excitation was considered to be CT if at least 10 pp of the electron density was transferred from the trimer to PC₇₁BM.

Excited state properties of the O3p–PC₇₁BM models with the minimized intermolecular distances

Table S11 Oscillator strengths for the first 10 singlet excited states of the O3p–PC₇₁BM models with the minimized intermolecular distance between the planarized O3p trimer and PC₇₁BM.

Model	Functional	S ₁	S ₂	S ₃	S ₄	S ₅	S ₆	S ₇	S ₈	S ₉	S ₁₀
1a	B3LYP	0.00	0.01	3.18	0.08	0.00	0.03	0.00	(0.00)	0.03	0.01
	ω B97X	0.00	5.28	0.05	0.07	0.05	0.03	0.00	0.01	0.03	0.00
	ω B97X-D	0.00	5.05	0.04	0.06	0.03	0.01	0.01	0.01	0.03	0.01
	OT- ω B97X	0.00	4.44	0.02	0.03	0.00	0.01	0.00	0.04	0.04	(0.00)
	OT- ω B97X-D	0.00	4.53	0.02	0.04	0.01	0.01	0.01	0.01	0.07	0.06
2a	B3LYP	0.02	0.04	3.04	0.18	0.00	0.01	0.03	0.00	(0.00)	(0.02)
	ω B97X	0.00	4.87	0.27	0.07	0.08	0.02	0.01	0.03	0.03	0.00
	ω B97X-D	0.01	4.63	0.14	0.08	0.06	0.01	0.08	0.01	0.06	0.01
	OT- ω B97X	0.00	4.41	0.02	0.03	0.01	0.01	0.00	0.10	0.05	(0.40)
	OT- ω B97X-D	0.03	4.22	0.03	0.10	0.00	0.15	0.02	0.06	(0.09)	0.14
3a	B3LYP	0.04	0.04	0.83	2.36	0.00	0.00	0.05	0.00	0.00	0.05
	ω B97X	0.00	4.41	0.60	0.10	0.09	0.02	0.01	0.06	0.04	0.00
	ω B97X-D	0.01	4.41	0.26	0.10	0.08	0.01	0.01	0.11	0.07	0.00
	OT- ω B97X	0.00	4.39	0.02	0.03	0.01	0.01	0.00	(0.16)	0.05	0.35
	OT- ω B97X-D	0.05	4.01	0.08	0.16	0.01	0.24	0.02	0.09	(0.16)	0.03
1b	B3LYP	0.00	0.00	3.15	0.01	0.00	0.04	0.00	0.13	0.00	0.01
	ω B97X	0.00	5.17	0.08	0.13	0.02	0.03	0.01	0.01	0.02	0.00
	ω B97X-D	0.00	4.98	0.04	0.10	0.02	0.01	0.03	0.00	0.03	0.00
	OT- ω B97X	0.00	4.38	0.02	0.03	0.00	0.01	0.00	(0.06)	0.07	0.47
	OT- ω B97X-D	0.00	4.47	0.01	0.02	0.04	0.00	0.02	0.00	(0.14)	(0.02)
2b	B3LYP	0.01	0.01	3.15	0.06	0.00	0.03	0.00	0.00	0.03	0.01
	ω B97X	0.00	4.95	0.12	0.14	0.03	0.03	0.00	0.04	0.06	0.00
	ω B97X-D	0.01	4.73	0.04	0.14	0.01	0.01	0.05	0.10	0.04	0.00
	OT- ω B97X	0.00	4.37	0.02	0.04	0.00	0.01	0.00	0.05	0.09	0.46
	OT- ω B97X-D	0.02	4.26	0.01	0.13	0.07	0.00	0.01	0.00	(0.08)	0.04
3b	B3LYP	0.03	0.06	3.13	0.06	0.00	0.00	0.04	0.00	0.00	0.02
	ω B97X	0.00	4.78	0.22	0.10	0.05	0.06	0.02	0.04	0.08	0.00
	ω B97X-D	0.00	4.59	0.05	0.12	0.05	0.01	0.16	0.05	0.08	0.02
	OT- ω B97X	0.00	4.38	0.02	0.03	0.00	0.01	0.00	(0.07)	0.07	0.43
	OT- ω B97X-D	0.04	3.75	0.01	0.49	0.09	0.22	0.04	0.00	0.07	0.03

The oscillator strengths that are greater than or equal to 0.10 are in bold. The oscillator strengths of the excited singlet states that did not converge are in parenthesis.

Table S12 Vertical transition energies (eV) for the first 10 singlet excited states of the O3p–PC₇₁BM models with the minimized intermolecular distance between the planarized O3p trimer and PC₇₁BM.

Model	Functional	S ₁	S ₂	S ₃	S ₄	S ₅	S ₆	S ₇	S ₈	S ₉	S ₁₀
1a	B3LYP	1.63	1.69	1.74	1.76	1.88	1.92	1.94	(2.01)	2.02	2.03
	ωB97X	2.40	2.67	2.69	2.83	2.86	2.93	2.94	2.96	3.02	3.04
	ωB97X-D	2.28	2.48	2.52	2.66	2.68	2.73	2.77	2.78	2.81	2.85
	OT-ωB97X	2.13	2.19	2.26	2.37	2.39	2.45	2.47	2.52	2.53	(2.56)
	OT-ωB97X-D	2.15	2.21	2.29	2.39	2.41	2.43	2.49	2.50	2.55	2.56
2a	B3LYP	1.63	1.69	1.74	1.77	1.86	1.92	1.92	2.00	(2.01)	(2.02)
	ωB97X	2.40	2.66	2.68	2.83	2.86	2.92	2.94	2.95	3.02	3.03
	ωB97X-D	2.28	2.46	2.51	2.66	2.68	2.72	2.76	2.76	2.81	2.85
	OT-ωB97X	2.13	2.19	2.26	2.37	2.39	2.45	2.47	2.52	2.53	(2.55)
	OT-ωB97X-D	2.15	2.20	2.29	2.39	2.43	2.45	2.48	2.50	(2.55)	2.56
3a	B3LYP	1.60	1.66	1.73	1.75	1.83	1.89	1.92	1.96	2.01	2.02
	ωB97X	2.40	2.65	2.68	2.83	2.85	2.92	2.93	2.95	3.02	3.03
	ωB97X-D	2.28	2.46	2.51	2.66	2.68	2.72	2.76	2.77	2.80	2.85
	OT-ωB97X	2.13	2.19	2.25	2.37	2.39	2.45	2.47	(2.52)	2.53	2.55
	OT-ωB97X-D	2.15	2.19	2.28	2.38	2.42	2.47	2.48	2.50	(2.54)	2.56
1b	B3LYP	1.64	1.69	1.73	1.80	1.91	1.93	1.96	2.00	2.01	2.03
	ωB97X	2.40	2.67	2.68	2.82	2.86	2.92	2.93	2.96	3.01	3.03
	ωB97X-D	2.28	2.48	2.51	2.65	2.69	2.72	2.74	2.78	2.80	2.85
	OT-ωB97X	2.13	2.19	2.25	2.37	2.39	2.45	2.47	2.52	2.53	2.55
	OT-ωB97X-D	2.15	2.21	2.28	2.35	2.39	2.42	2.48	2.50	2.55	2.56
2b	B3LYP	1.63	1.68	1.74	1.78	1.88	1.92	1.93	2.01	2.02	2.03
	ωB97X	2.40	2.66	2.68	2.82	2.86	2.91	2.93	2.95	3.00	3.03
	ωB97X-D	2.29	2.47	2.52	2.65	2.68	2.72	2.75	2.77	2.78	2.85
	OT-ωB97X	2.13	2.19	2.25	2.37	2.39	2.45	2.47	2.52	2.53	2.55
	OT-ωB97X-D	2.15	2.20	2.29	2.38	2.40	2.42	2.48	2.49	2.55	(2.57)
3b	B3LYP	1.61	1.66	1.75	1.76	1.84	1.89	1.92	1.98	2.01	2.03
	ωB97X	2.40	2.66	2.68	2.83	2.86	2.92	2.93	2.96	3.00	3.03
	ωB97X-D	2.28	2.47	2.51	2.66	2.68	2.73	2.75	2.78	2.79	2.85
	OT-ωB97X	2.13	2.19	2.25	2.37	2.39	2.45	2.47	(2.52)	2.53	2.55
	OT-ωB97X-D	2.15	2.19	2.28	2.37	2.41	2.43	2.48	2.50	2.55	2.56

The transitions, whose oscillator strengths (Table S11) are greater than or equal to 0.10, are in bold. The values of the excited singlet states that did not converge are in parenthesis.

Table S13 Nature of the first 10 singlet excited states of the O3p–PC₇₁BM models with the minimized intermolecular distance between the planarized O3p trimer and PC₇₁BM.

Model	Functional	S ₁	S ₂	S ₃	S ₄	S ₅	S ₆	S ₇	S ₈	S ₉	S ₁₀
1a	B3LYP	PCT	PCT	LT	PCT	PCT	LT	PCT	(LF)	CT	PCT
	ωB97X	LF	LT	LF	LF	LT	LF	LF	LF	LF	LF
	ωB97X-D	LF	LT	LF	LT	LF	LF	LF	LF	LF	LF
	OT-ωB97X	LF	LT	LF	LT	LF	LF	LF	LF	LF	(LF)
	OT-ωB97X-D	LF	LT	LF	LT	CT	LF	LF	LF	LF	LF
2a	B3LYP	PCT	PCT	LT	PCT	PCT	PCT	LT	PCT	(LF)	(CT)
	ωB97X	LF	LT	LF	LF	LT	LF	LF	LF	LF	LF
	ωB97X-D	LF	LT	LF	LT	LF	LF	LF	LF	LF	LF
	OT-ωB97X	LF	LT	LF	LT	LF	LF	LF	LF	LF	LT
	OT-ωB97X-D	LF	LT	LF	LT	LF	CT	LF	LF	(LF)	CT
3a	B3LYP	PCT	PCT	CT	CT	PCT	PCT	LT	PCT	LF	LT
	ωB97X	LF	LT	LF	LF	LT	LF	LF	LF	LF	LF
	ωB97X-D	LF	LT	LF	LT	LF	LF	LF	LF	LF	LF
	OT-ωB97X	LF	LT	LF	LT	LF	LF	LF	(LF)	LF	LT
	OT-ωB97X-D	LF	LT	LF	LT	LF	CT	LF	LF	(LF)	LF
1b	B3LYP	PCT	PCT	LT	PCT	PCT	LT	PCT	LT	LF	LF
	ωB97X	LF	LT	LF	LF	LT	LF	LF	LF	LF	LF
	ωB97X-D	LF	LT	LF	LT	LF	LF	LF	LF	LF	LF
	OT-ωB97X	LF	LT	LF	LT	LF	LF	LF	LF	LF	LT
	OT-ωB97X-D	LF	LT	LF	CT	LT	LF	LF	LF	LF	LF
2b	B3LYP	PCT	PCT	LT	PCT	PCT	LT	PCT	LF	CT	LF
	ωB97X	LF	LT	LF	LF	LT	LF	LF	LF	LF	LF
	ωB97X-D	LF	LT	LF	LT	LF	LF	LF	LF	LF	LF
	OT-ωB97X	LF	LT	LF	LT	LF	LF	LF	LF	LF	LT
	OT-ωB97X-D	LF	LT	LF	CT	CT	LF	LF	LF	(LF)	LF
3b	B3LYP	PCT	PCT	LT	PCT	PCT	PCT	LT	PCT	LF	LF
	ωB97X	LF	LT	LF	LF	LT	LF	LF	LF	LF	LF
	ωB97X-D	LF	LT	LF	LT	LF	LF	LF	LF	LF	LF
	OT-ωB97X	LF	LT	LF	LT	LF	LF	LF	(LF)	LF	LT
	OT-ωB97X-D	LF	CT	LF	CT	LF	CT	LF	LF	LF	LF

Only the NTO pair with the largest λ , i.e. the fraction of the NTO pair contribution to the particular excitation has been considered. The transitions, whose oscillator strengths (Table S11) are greater than or equal to 0.10, are in bold. The results of the excited singlet states that did not converge are in parenthesis. PCT: ‘pure’ charge transfer from the O3p trimer to PC₇₁BM, i.e. ≥ 90 pp of the electron density was transferred; CT: charge transfer from the O3p trimer to PC₇₁BM, i.e. 10 pp < of the electron density < 90 pp was transferred; LT: local excitation in the O3p trimer. LF: local excitation in PC₇₁BM. The threshold was 10 pp, i.e. excitation was considered to be CT if at least 10 pp of the electron density was transferred from the trimer to PC₇₁BM.

UV-Vis absorption spectra of O3p, PC₇₁BM, and the models 3a and 3b

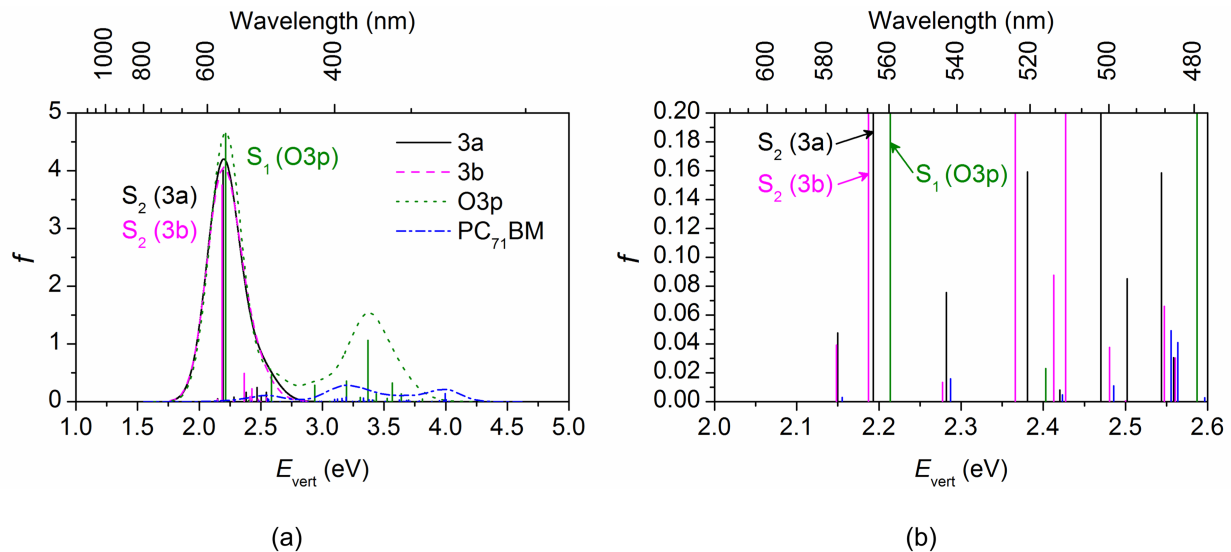


Figure S9 (a) Vertical transition energies and the corresponding UV-vis absorption spectra of O3p, PC₇₁BM, and O3p-PC₇₁BM models (**3a** and **3b** with the optimal intermolecular distances) calculated in vacuum with TDDFT at the OT- ω B97X-D/6-31G** level of theory. (b) A close-up of the region including the first 10 singlet vertical transitions of **3a** and **3b**. Here, the ω of 0.12 bohr⁻¹ (i.e. the optimal ω of the O3p-PC₇₁BM models) was employed in all calculations for consistency. The geometries optimized at the DFT/B3LYP/6-31G** level of theory were used. Experimental absorption maxima³ of copolymer-PC₇₁BM (1:1) blend film is at ca. 560–570 nm (2.18–2.21 eV).

Natural transition orbitals of the vertical model 3a at the intermolecular distance of 3.5 Å

B3LYP

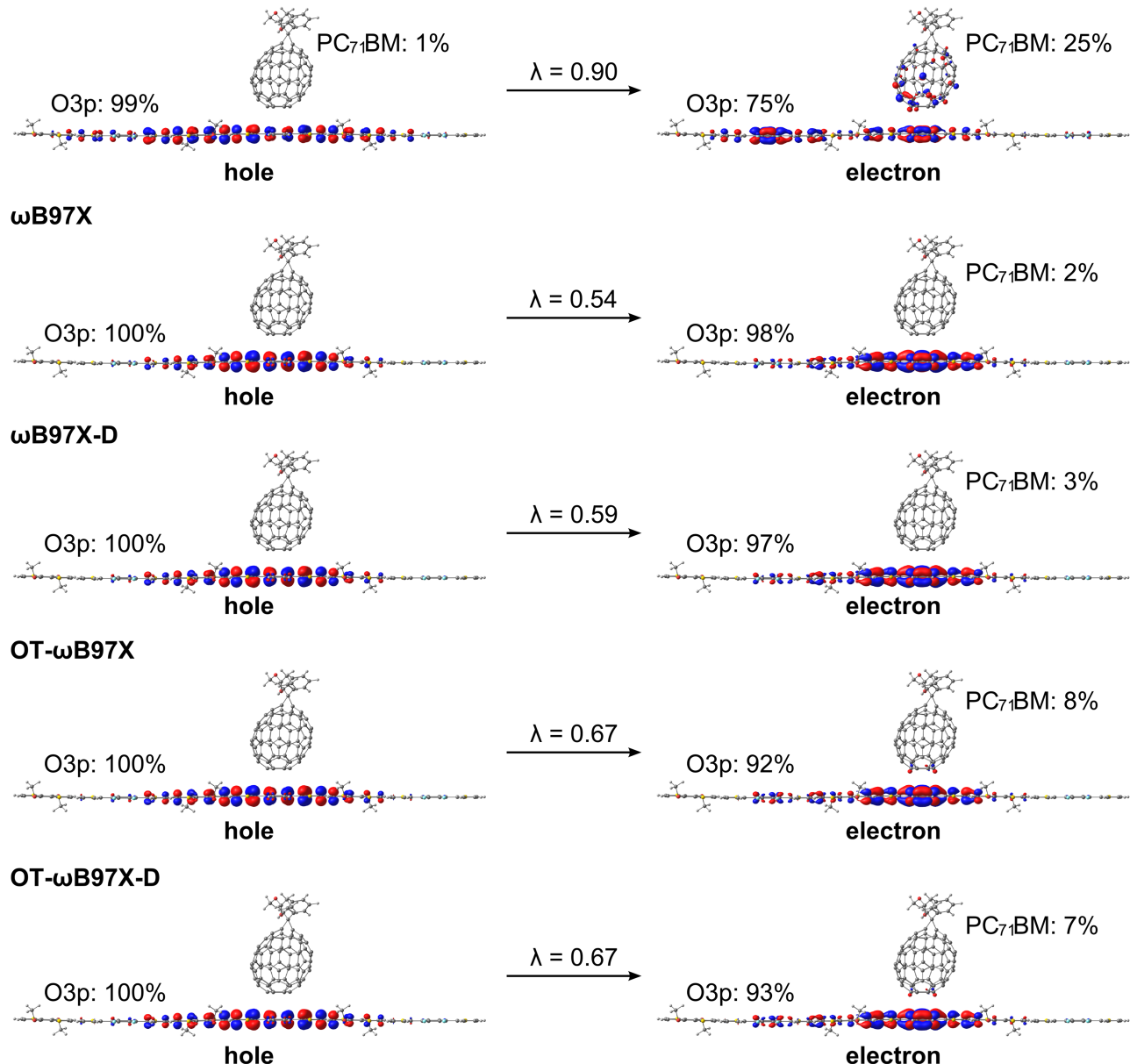


Figure S10 NTOs for the transition maximum (B3LYP: $S_0 \rightarrow S_4$, other functionals: $S_0 \rightarrow S_2$) of the vertical model **3a** calculated with different functionals and the 6-31G** basis set (isodensity contour = 0.025). The distance between O3p and PC71BM was set at 3.5 Å. In addition, the contributions (%) of O3p and PC71BM to the NTOs and contributions (λ) of the NTO pair to particular excitation are presented.

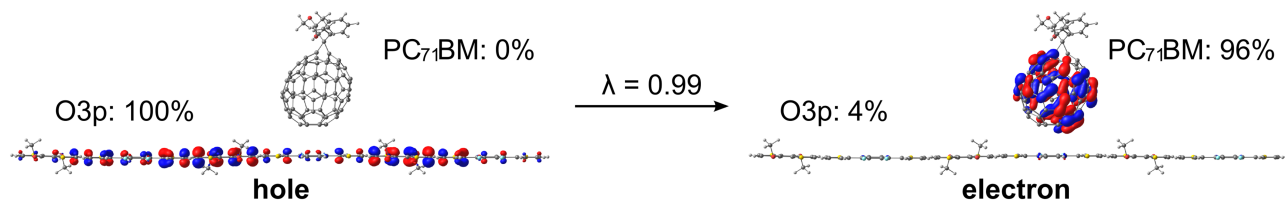
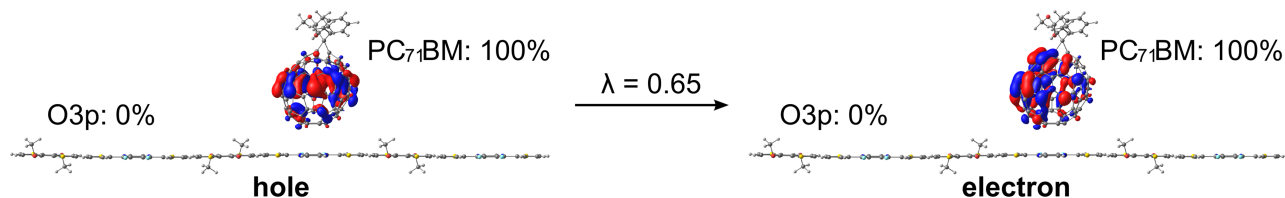
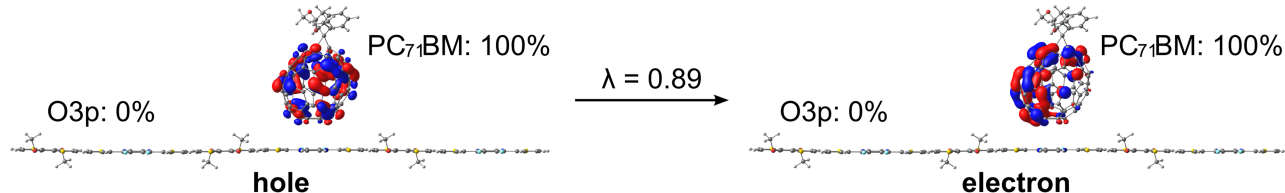
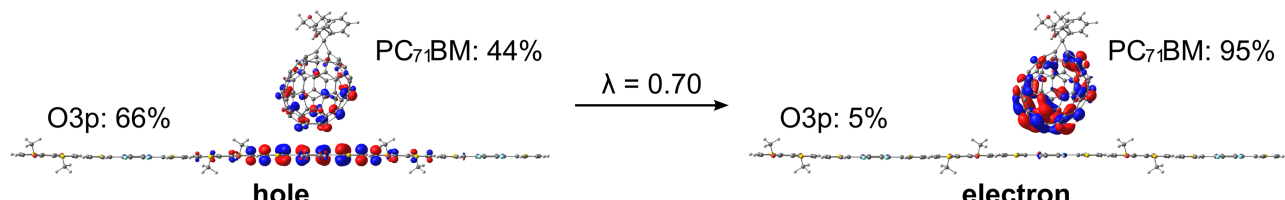
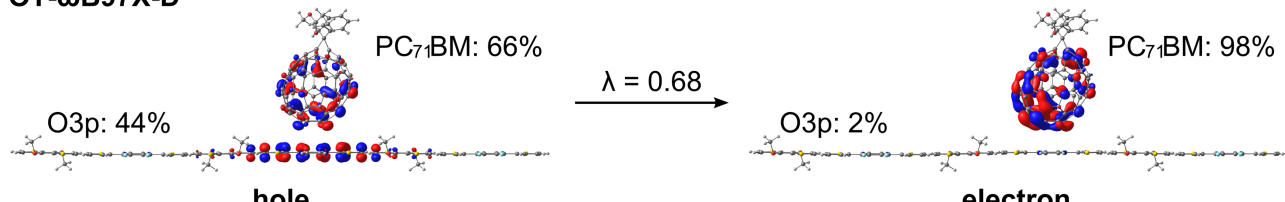
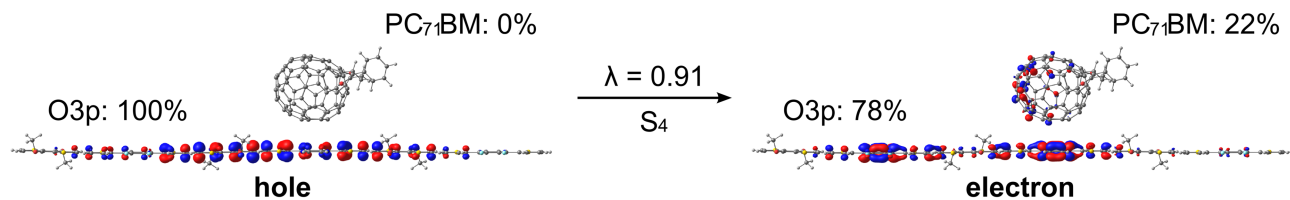
B3LYP **ω B97X** **ω B97X-D****OT- ω B97X****OT- ω B97X-D**

Figure S11 NTOs for the $S_0 \rightarrow S_6$ transition of the vertical model **3a** calculated with different functionals and the 6-31G** basis set (isodensity contour = 0.025). The distance between O3p and PC₇₁BM was set at 3.5 Å. In addition, the contributions (%) of O3p and PC₇₁BM to the NTOs and contributions (λ) of the NTO pair to particular excitation are presented.

Natural transition orbitals of the horizontal model **3b** at the intermolecular distance of 3.5 Å

B3LYP



OT- ω B97X-D

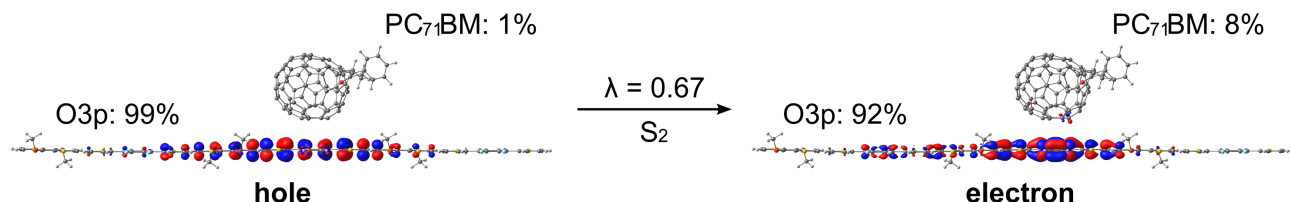
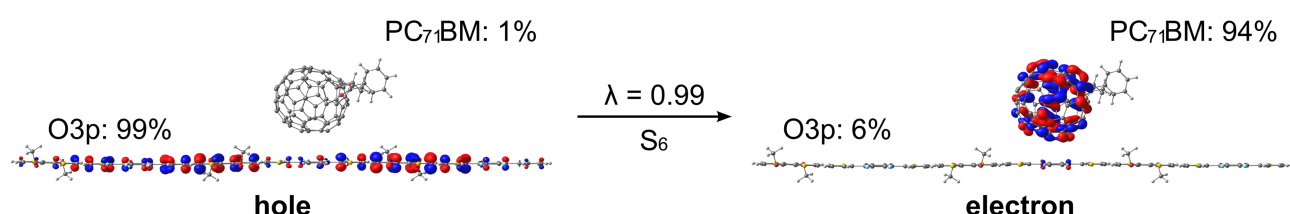


Figure S12 NTOs for the transition maximum of the horizontal model **3b** calculated with different functionals and the 6-31G** basis set (isodensity contour = 0.025). The distance between O3p and PC₇₁BM was set at 3.5 Å. In addition, the contributions (%) of O3p and PC₇₁BM to the NTOs and contributions (λ) of the NTO pair to particular excitation are presented.

B3LYP



OT- ω B97X-D

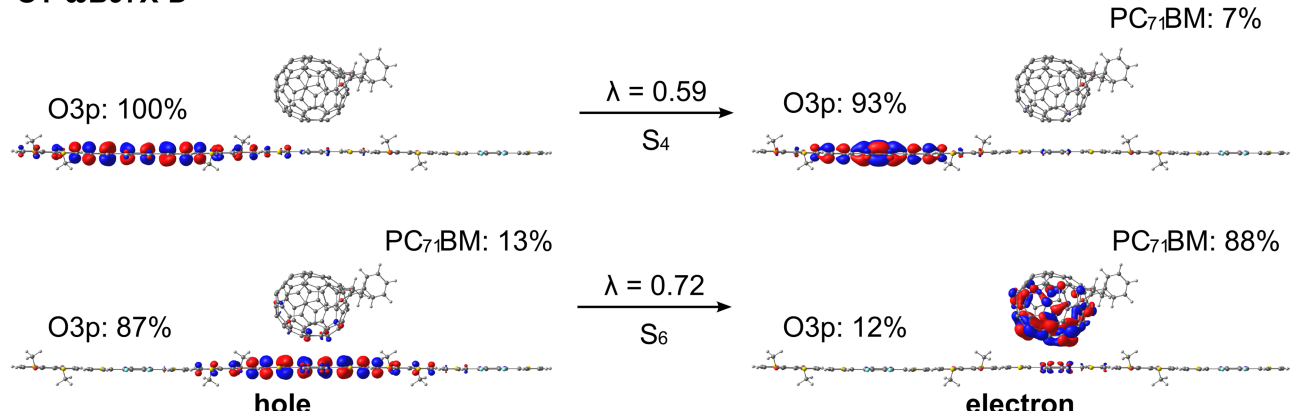


Figure S13 NTOs for additional singlet vertical transitions of the horizontal model **3b** calculated with different functionals and the 6-31G** basis set (isodensity contour = 0.025). The distance between O3p and PC₇₁BM was set at 3.5 Å. In addition, the contributions (%) of O3p and PC₇₁BM to the NTOs and contributions (λ) of the NTO pair to particular excitation are presented.

References

- 1 M. M. Wienk, J. M. Kroon, W. J. H. Verhees, J. Knol, J. C. Hummelen, P. A. van Hal and R. A. J. Janssen, *Angew. Chem. Int. Ed.*, 2003, **42**, 3371–3375.
- 2 W. H. Powell, F. Cozzi, G. P. Moss, C. Thilgen, R. J.-R. Hwu and A. Yerin, *Pure Appl. Chem.*, 2002, **74**, 629–695.
- 3 H.-C. Chen, Y.-H. Chen, C.-C. Liu, Y.-C. Chien, S.-W. Chou and P.-T. Chou, *Chem. Mater.*, 2012, **24**, 4766–4772.
- 4 P. Ros and G. C. A. Schuit, *Theor. Chim. Acta*, 1966, **4**, 1–12.
- 5 Q. Bao, O. Sandberg, D. Dagnelund, S. Sandén, S. Braun, H. Aarnio, X. Liu, W. M. Chen, R. Österbacka and M. Fahlman, *Adv. Funct. Mater.*, 2014, **24**, 6309–6316.
- 6 H. Yoshida, *J. Phys. Chem. C*, 2014, **118**, 24377–24382.
- 7 K. Akaike, K. Kanai, H. Yoshida, J. Tsutsumi, T. Nishi, N. Sato, Y. Ouchi and K. Seki, *J. Appl. Phys.*, 2008, **104**, 023710.
- 8 B. W. Larson, J. B. Whitaker, X.-B. Wang, A. A. Popov, G. Rumbles, N. Kopidakis, S. H. Strauss and O. V. Boltalina, *J. Phys. Chem. C*, 2013, **117**, 14958–14964.